Electronic Supplementary Material (ESI) for Dalton Transactions

Electronic supplementary information (ESI)

for

Lanthanide(III) complexes of aminoethyl-DO3A as PARACEST contrast agents based on decoordination of the weakly bound amino group

Tereza Krchová,[a] Jan Kotek,[a]* Daniel Jirák,[b] Jana Havlíčková,[a] Ivana Císařová,[a] Petr Hermann[a]

[a] *Department of Inorganic Chemistry, Universita Karlova (Charles University), Hlavova 2030, 128 40 Prague 2, Czech Republic. Tel: +420-22195-1261. Fax: +420-22195-1253. E-mail: modrej@natur.cuni.cz.*

[b] *Department of Radiodiagnostic and Interventional Radiology, Magnetic Resonance Unit, Institute of Clinical and Experimental Medicine, Vídeňská 1958/9, 140 21 Prague 4, Czech Republic.*

Content:

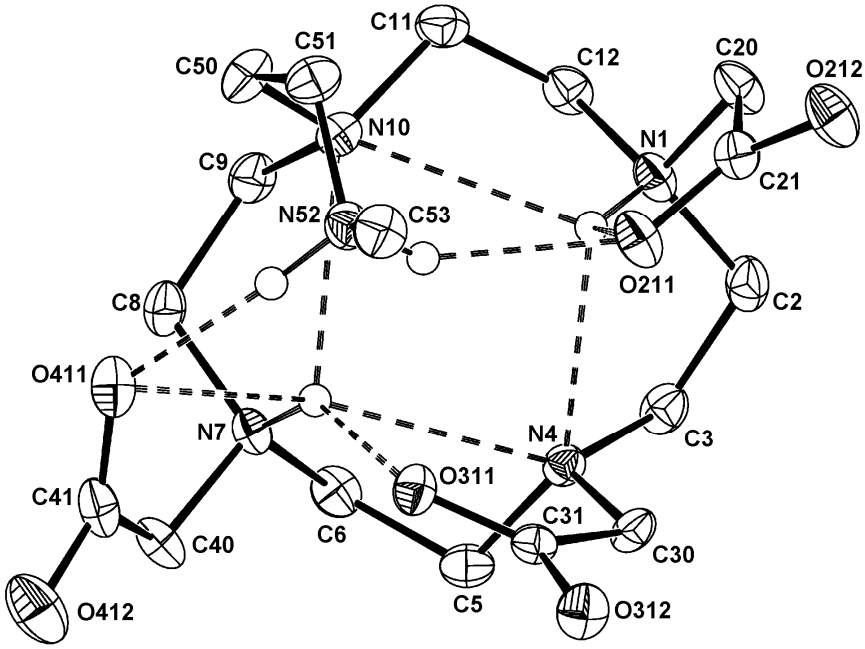

Fig. S1 Molecular structure of $H_3\mathbf{L}^2$ found in the crystal structure of $H_3\mathbf{L}^2{\cdot}6H_2O$. Dashed lines show system of intramolecular hydrogen bonds. Carbon-bound hydrogen atoms are omitted for sake of clarity.

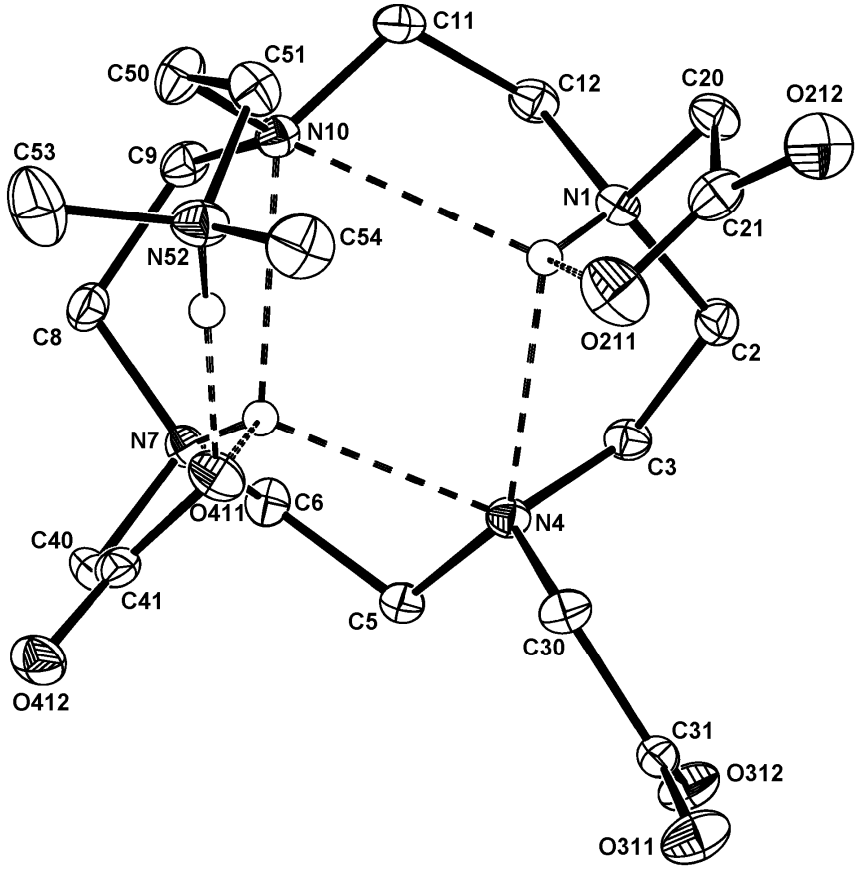

Fig. S2 Molecular structure of $H_3\mathbf{L}^3$ found in the crystal structure of $H_3\mathbf{L}^3{\cdot}3.5H_2O$. Dashed lines show system of intramolecular hydrogen bonds. Carbon-bound hydrogen atoms are omitted for sake of clarity.

Table S1 Torsion angles in the macrocyclic units found in the crystal structures of $H_3\mathbf{L}^1 \cdot 5H_2O$, $H_3\mathbf{L}^2 \cdot 6H_2O$ and $H_3\mathbf{L}^3 \cdot 3.5H_2O$.

Torsion angle, °	$H_3\mathbf{L}^1$	$H_3\mathbf{L}^2$	$H_3\mathbf{L}^3$
N1-C2-C3-N4	–49.71(13)	–47.30(16)	–53.54(13)
C2-C3-N4-C5	170.56(10)	168.61(12)	166.59(9)
C3-N4-C5-C6	–88.19(11)	–90.39(14)	–90.36(11)
N4-C5-C6-N7	–63.19(12)	–64.59(15)	–58.02(12)
C5-C6-N7-C8	153.42(10)	154.47(11)	159.90(9)
C6-N7-C8-C9	–73.43(12)	–73.59(14)	–76.06(12)
N7-C8-C9-N10	–58.24(13)	–55.17(16)	–58.50(13)
C8-C9-N10-C11	167.89(10)	167.82(12)	163.69(9)
C9-N10-C11-C12	–78.57(12)	–78.52(14)	–80.67(11)
N10-C11-C12-N1	–62.61(12)	–67.48(14)	–68.79(12)
C11-C12-N1-C2	159.05(9)	158.99(11)	160.83(9)
C12-N1-C2-C3	–76.48(12)	–73.82(15)	–66.10(12)

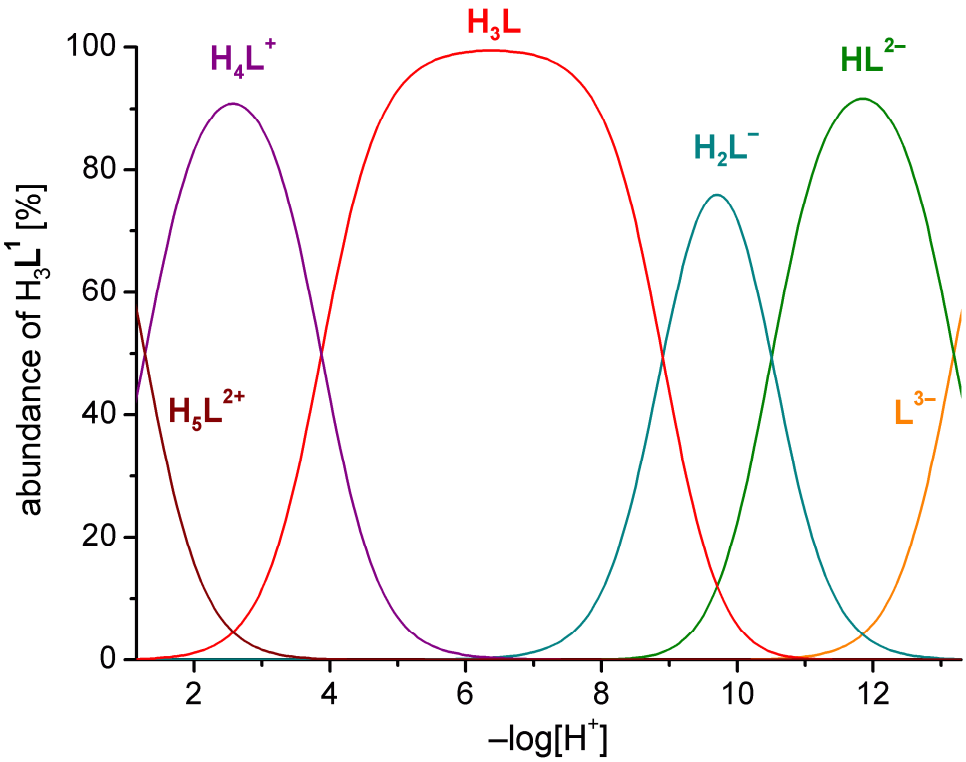

Fig. S3 The distribution diagram of $H_3\mathbf{L}^1$.

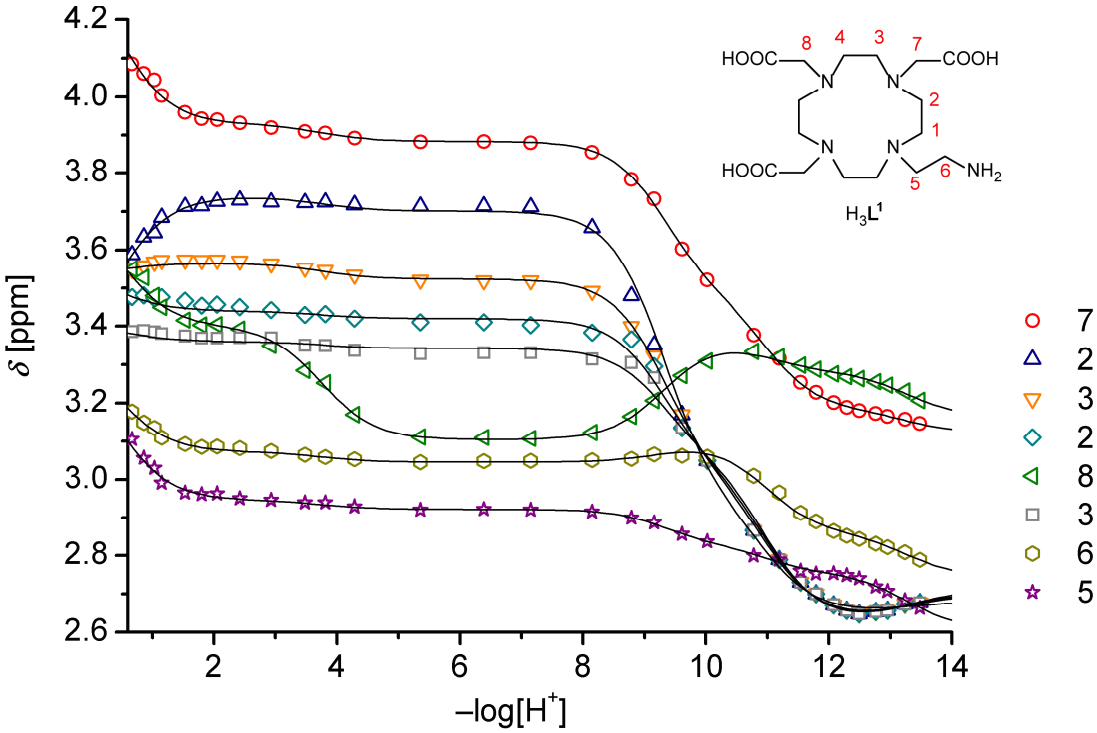

Fig. S4 pH dependence of d_H of $H_3\mathbf{L^1}$ (B_0 = 14.1 T, 25 °C). Dependence of chemical shifts of protons 1 and 4 were not included as they are overlapping with other signals. At pH below 9, individual protons of CH_2 groups 2 and 3 became nonequivalent resulting in two signals for each of groups.

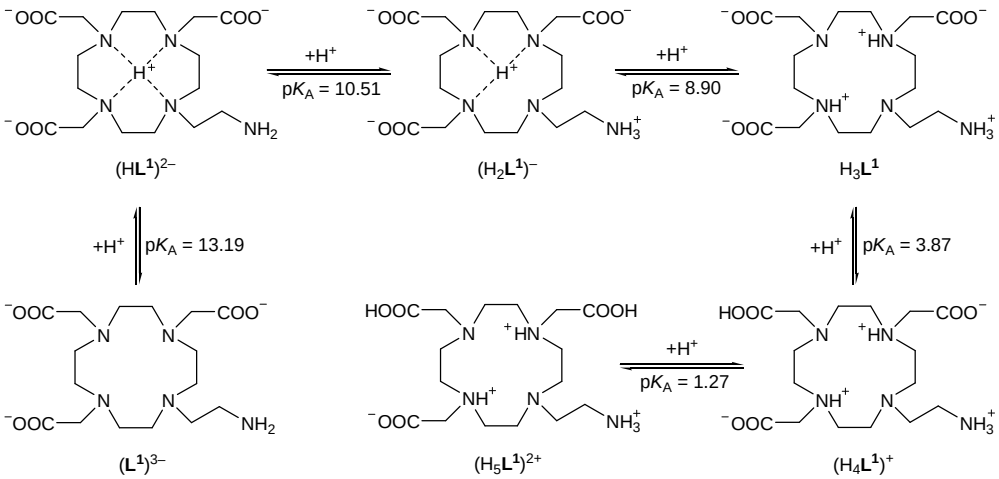

Scheme S1 Consecutive protonation scheme of $H_3\mathbf{L^1}$.

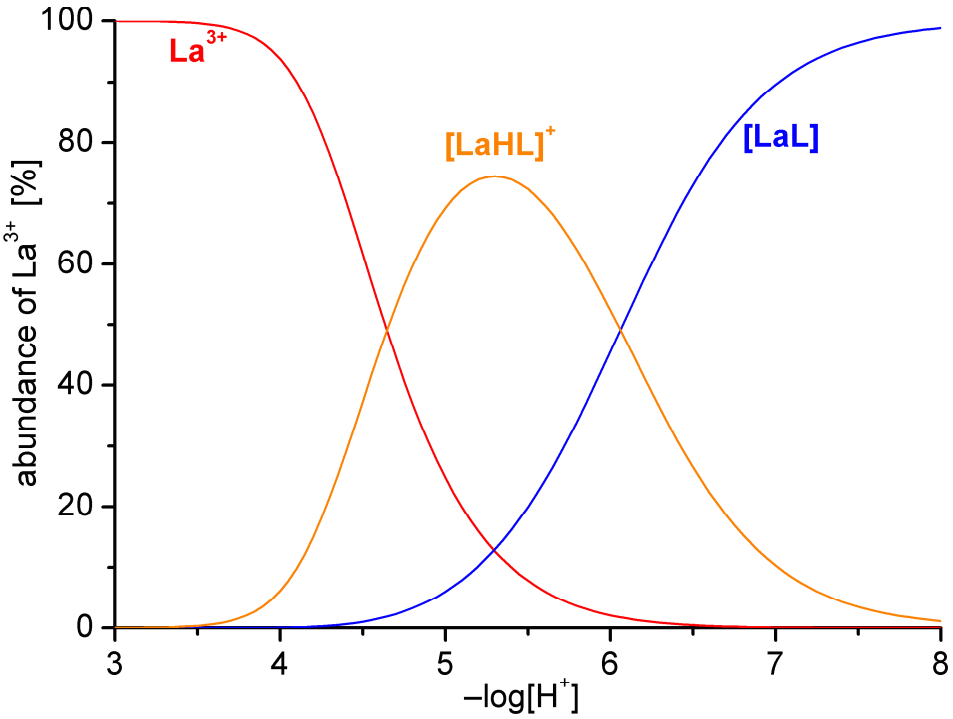

Fig. S5 Distribution diagram of the La^{3+}:H_3**L**^{1} ($c_M = c_L = 0.004$ M) system ($I = 0.1$ M (NMe_4)Cl, 25 °C); determined by potentiometry, L = (**L**^{1})$^{3-}$.

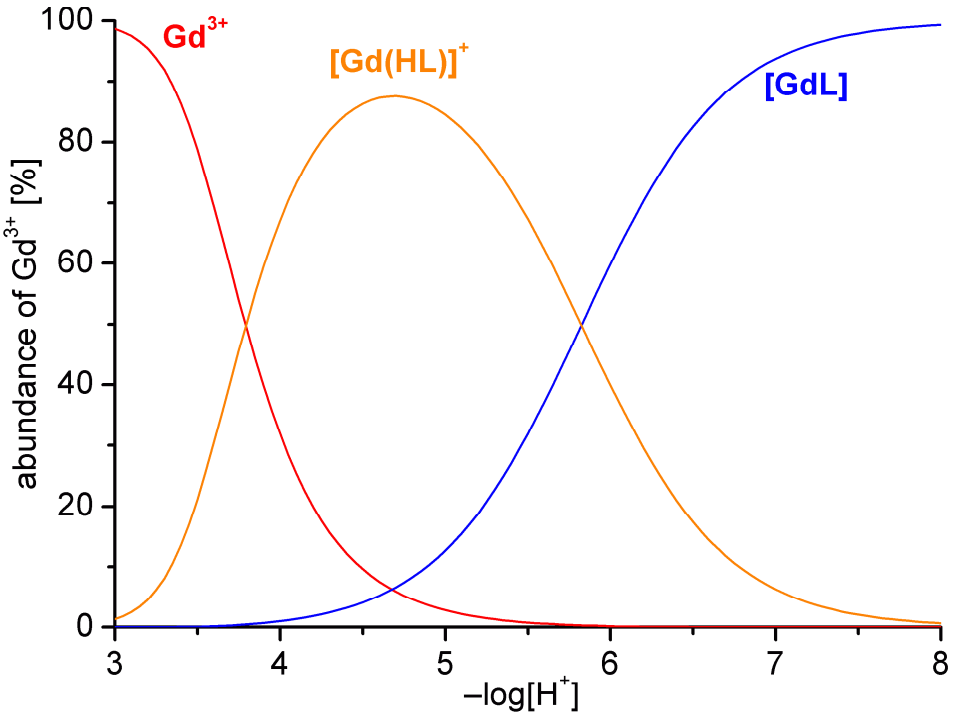

Fig. S6 Distribution diagram of the Gd^{3+}:H_3**L**^{1} ($c_M = c_L = 0.004$ M) system ($I = 0.1$ M (NMe_4)Cl, 25 °C); determined by potentiometry, L = (**L**^{1})$^{3-}$.

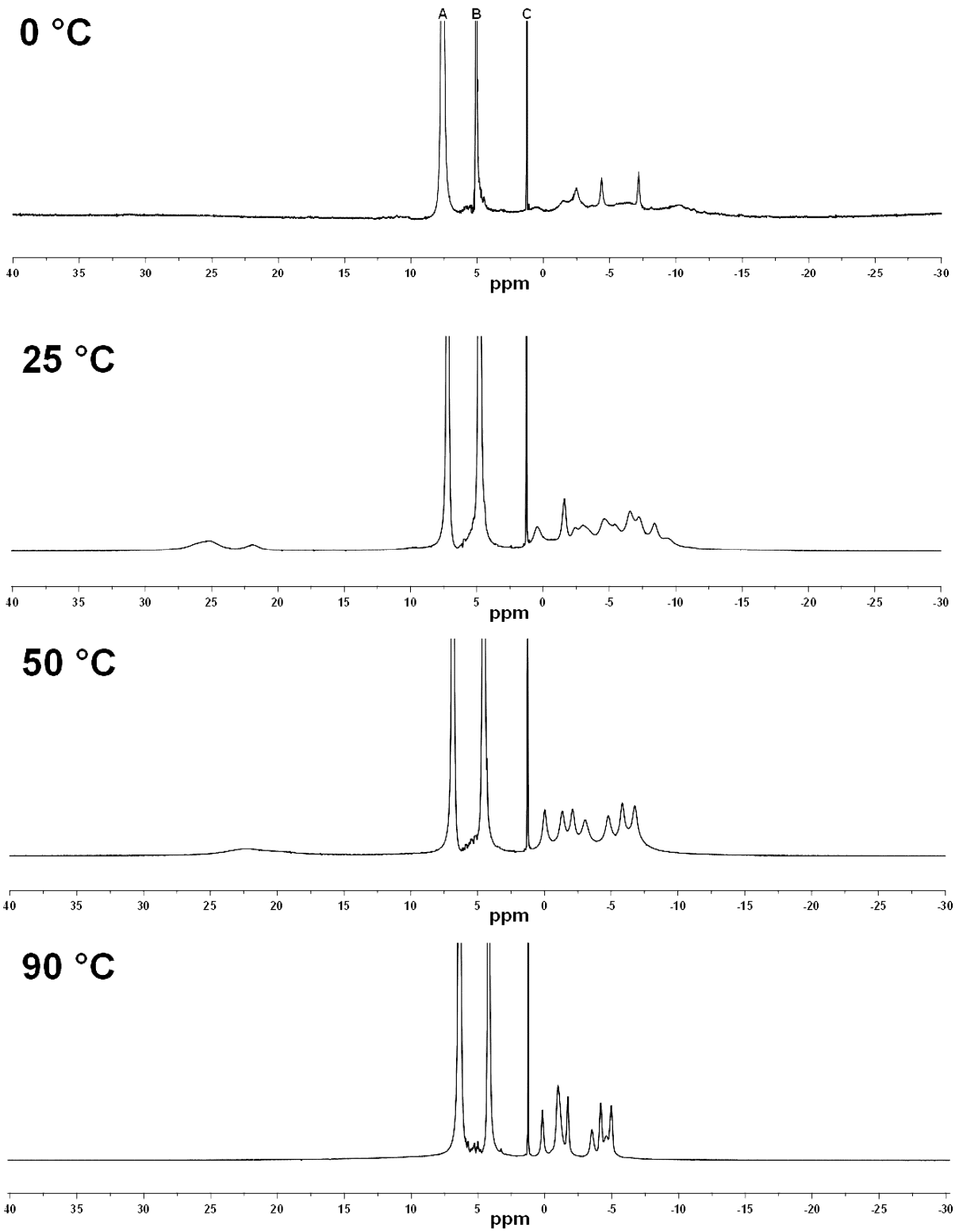

Fig. S7 ^{1}H NMR spectra of [Eu(H_2O)(**L**^{1})] (0.1 M solution in D_2O, B_0 = 7.05 T for 25, 50 and 90 °C and 9.4 T for 0 °C; pD = 9.0). A coaxial capillary with D_2O and *t*-BuOH was used as external standard (d_H = 1.25 ppm). Signals assignment: A = HDO in sample solution, B = HDO in capillary, C = *t*-BuOH in capillary

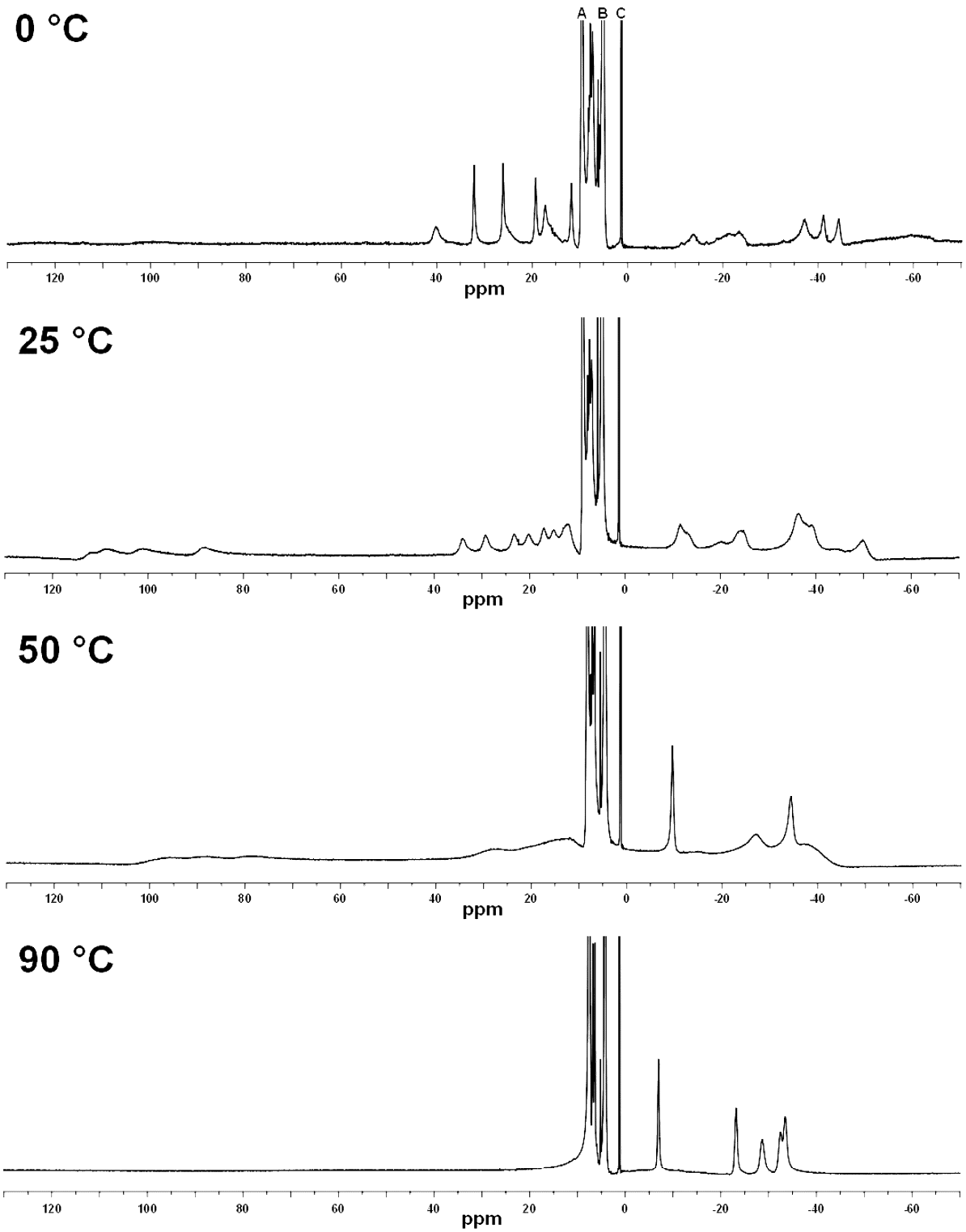

Fig. S8 ^{1}H NMR spectra of [Yb(**L**^{1})] (0.1 M solution in D_2O, B_0 = 7.05 T for 25, 50 and 90 °C and 9.4 T for 0 °C; pD = 8.5). A coaxial capillary with D_2O and *t*-BuOH was used as external standard (d_H = 1.25 ppm). Signals assignment: A = HDO in sample solution, B = HDO in capillary, C = *t*-BuOH in capillary.

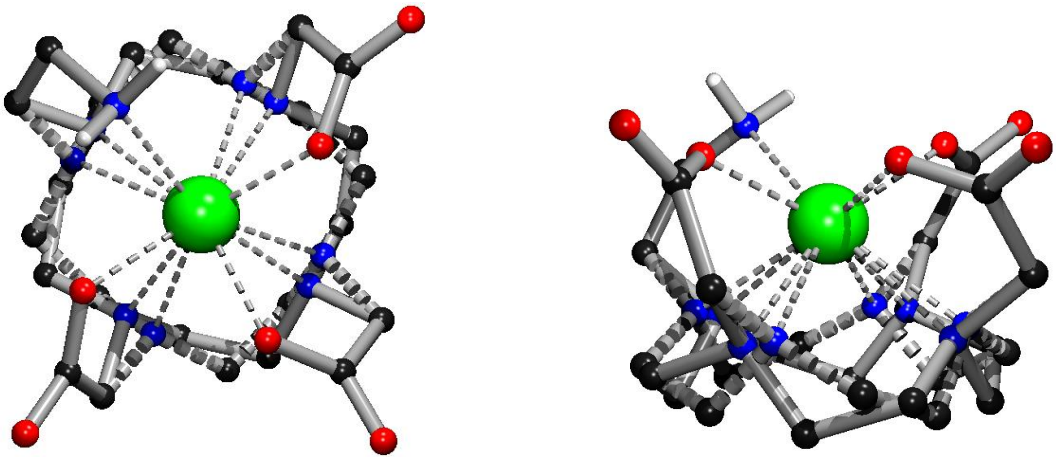

A **B**

Fig. S9 Disorder of the [Yb(**L**^{1})] molecule found in the solid-state structure of [Yb(**L**^{1})]·5H_2O. Figure shows overlay of both disordered complex species, more abundant (85 %) TSA' isomer is represented using solid bonds and less abundant (15 %) SA' isomer using dashed bonds. **A**: Top view. **B**: Side view. Carbon-bound hydrogen atoms are omitted for clarity reasons. Colour code: Yb – green; N – blue; O – red; C – black; H – grey.

Table S2 Geometric parameters of coordination sphere of Yb^{3+} ion in the crystal structure of [Yb(**L**^{1})]·5H_2O.

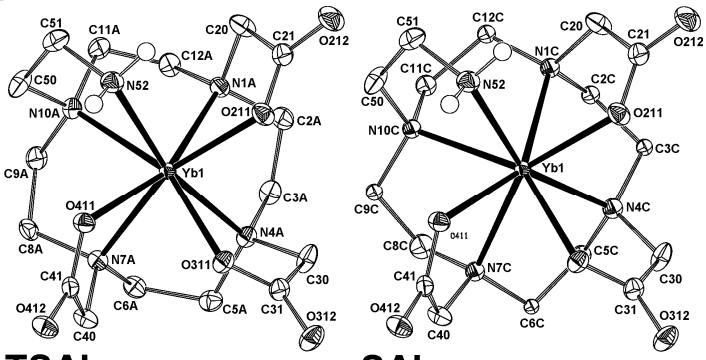

TSA' **SA'**

Coordination distances, Å		Distances from planes, Å	
N_4 plane of TSA' unit		NQA–OQ	2.5919
Yb1–N1A	2.519(2)	NQC–OQ	2.5042
Yb1–N4A	2.562(2)	Yb1–NQA	1.482(2)
Yb1–N7A	2.516(2)	Yb1–NQC	1.396(2)
Yb1–N10A	2.553(2)	Yb1–OQ	1.111(2)
N_4 plane of SA' unit		Dihedral angles of pendants in TSA' unit, °	
Yb1–N1C	2.535(12)	N1A-NQA-OQ-O211	–23.47(8)
Yb1–N4C	2.466(13)	N4A-NQA-OQ-O311	–23.90(8)
Yb1–N7C	2.498(13)	N7A-NQA-OQ-O411	–23.46(8)
Yb1–N10C	2.525(12)	N10A-NQA-OQ-N52	–19.15(8)
O_3N plane		Dihedral angles of pendants in SA' unit, °	
Yb1–O211	2.2707(12)	N1C-NQC-OQ-O211	–38.5(4)
Yb1–O311	2.2564(12)	N4C-NQC-OQ-O311	–38.8(4)
Yb1–O411	2.2764(12)	N7C-NQC-OQ-O411	–38.8(4)
Yb1–N52	2.4485(15)	N10C-NQC-OQ-N52	–34.3(4)

NQA – the centroid of the N_4-plane in TSA arrangement; NQC – the centroid of the N_4-plane in SA arrangement; OQ – the centroid of the O_3N-plane.

A

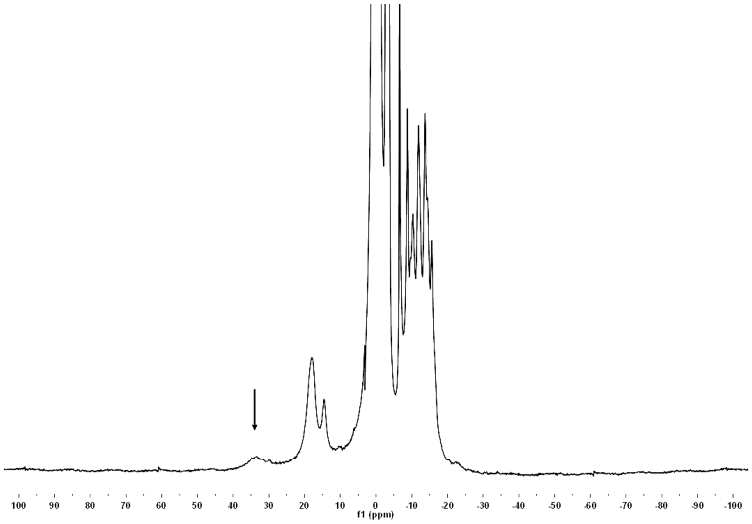

B

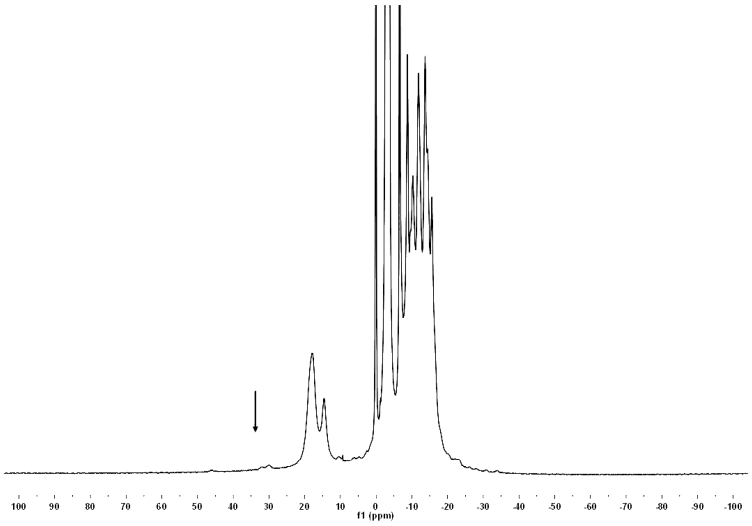

C

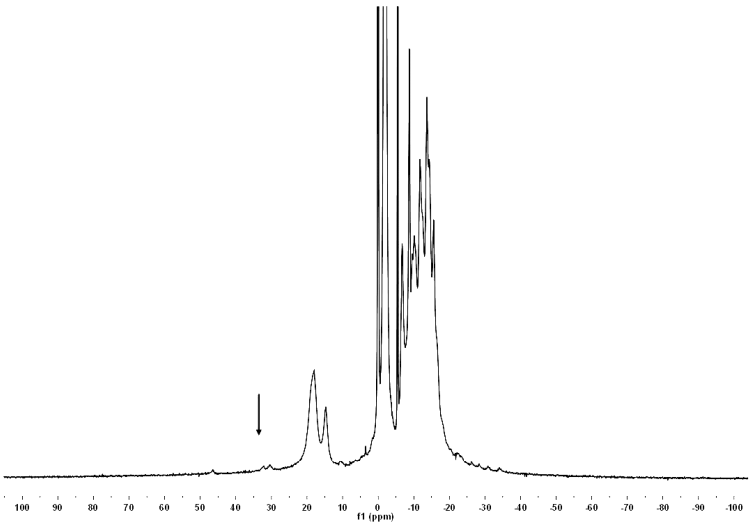

Fig. S10 A: ^{1}H NMR spectrum of [Eu(H_2O)(**L^1**)] (~1 M solution in H_2O, B_0 = 7.05 T, 25 °C, pH = 7.9). **B**: ^{1}H NMR spectrum of [Eu(H_2O)(**L^1**)] (~1 M solution in H_2O, B_0 = 7.05 T, 25 °C, pH = 7.9); water signal was saturated. **C**: ^{1}H NMR spectrum of [Eu(H_2O)(**L^1**)] (~1 M solution in D_2O, B_0 = 7.05 T, 25 °C, pD = 7.9). In all spectra, a coaxial capillary with D_2O and *t*-BuOH was used. Chemical shift of H_2O in solution was referenced to 0 ppm.

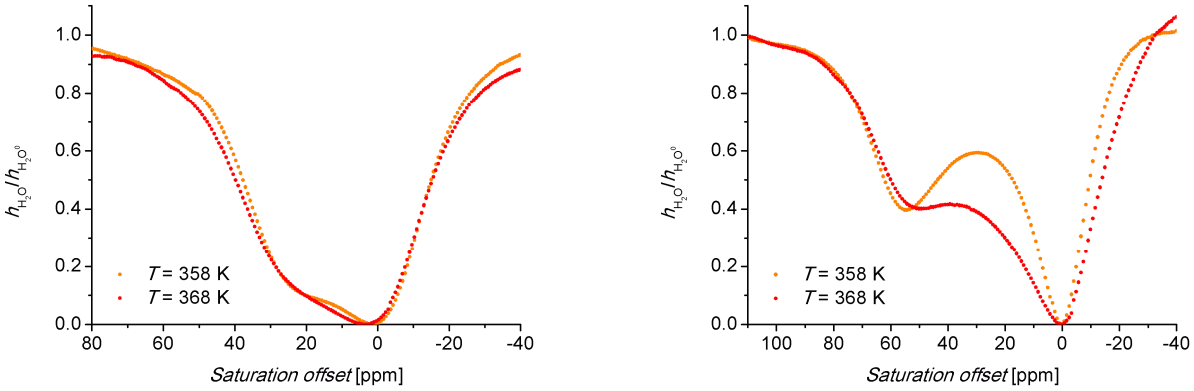

A **B**

Fig. S11 Z-spectra of 70 mM aq. solution of **A**: [Eu(H_2O)(**L**^{1})] and **B**: [Yb(**L**^{1})] complexes (B_0 = 7.05 T, satpwr = 29 dB (~1000 Hz), satdly = 2 s) at pH = 7.40.

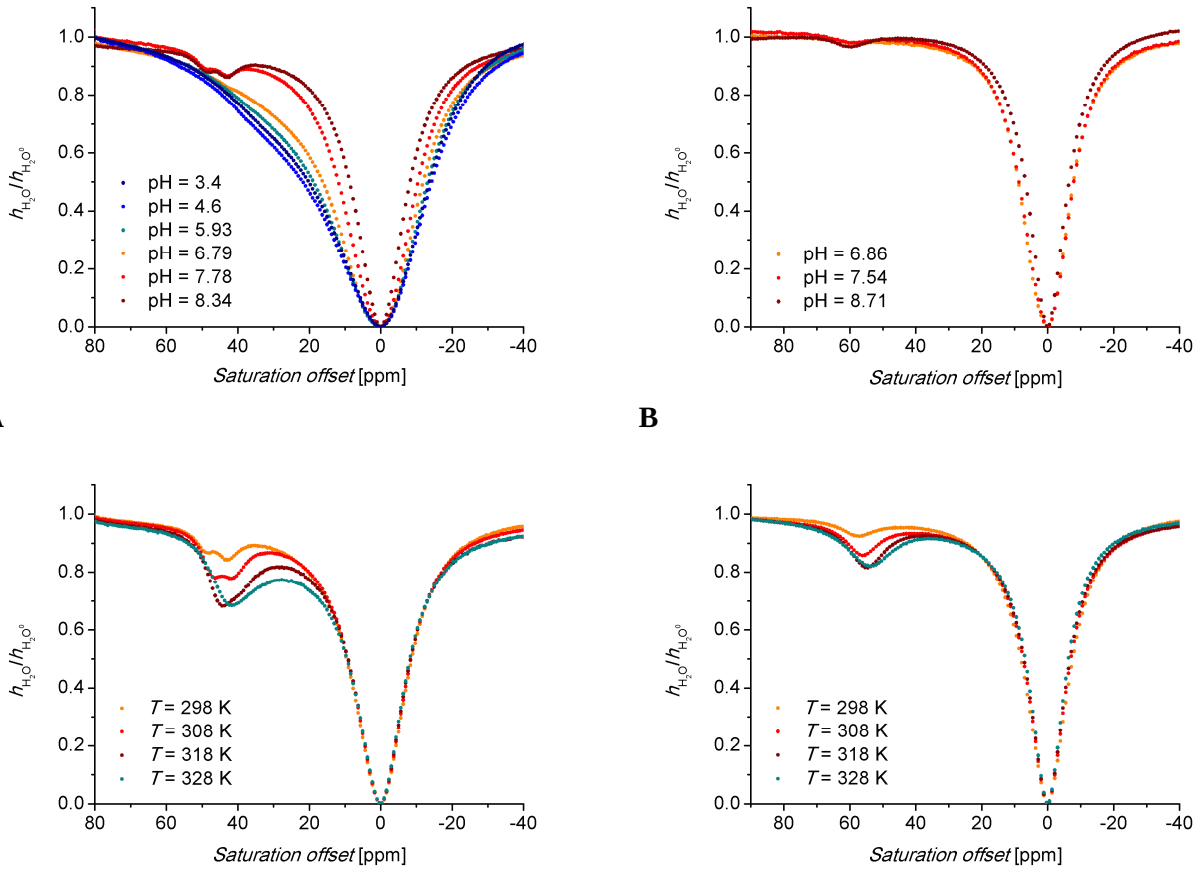

A **B**

C **D**

Fig. S12 A,**C**: Z-spectra of a 25 mM aq. solution (H_2O/D_2O 1:10) of [Eu(H_2O)(**L**^{2})] complex (B_0 = 7.05 T, satpwr = 29 dB~1000 Hz, satdly = 2 s). **A**: T = 298 K. **C**: pH = 8.16. **B**,**D**: Z-spectra of a 25 mM (**B**) or 50 mM (**D**) aq. solution (H_2O/D_2O 1:10) of [Yb(**L**^{2})] complex (B_0 = 7.05 T, satpwr = 29 dB~1000 Hz, satdly = 2 s). **B**: T = 298 K. **D**: pH = 8.35.

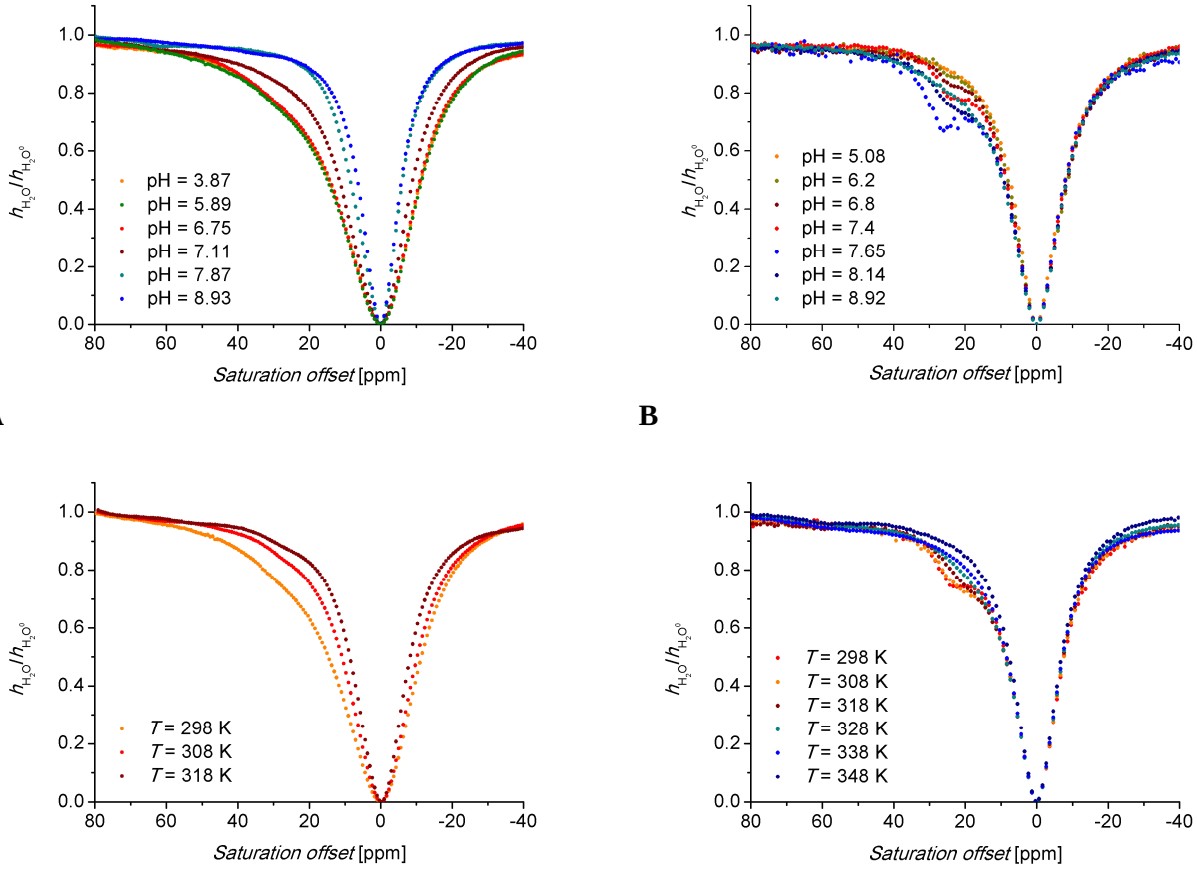

Fig. S13 A,**C**: Z-spectra of 25 mM aq. solution (H_2O/D_2O 1:10) of [Eu(H_2O)(**L**^{3})] complex (B_0 = 7.05 T, satpwr = 29 dB (~1000 Hz), satdly = 2 s); **A**: T = 298 K. **C**: pH = 5.40. **B**,**D**: Z-spectra of 50 mM aq. solutions (H_2O/D_2O 1:10) of the [Yb(**L**^{3})] complex (B_0 = 7.05 T, satpwr = 29 dB (~1000 Hz), satdly = 2 s); **B**: T = 298 K, **D**: pH = 7.72.

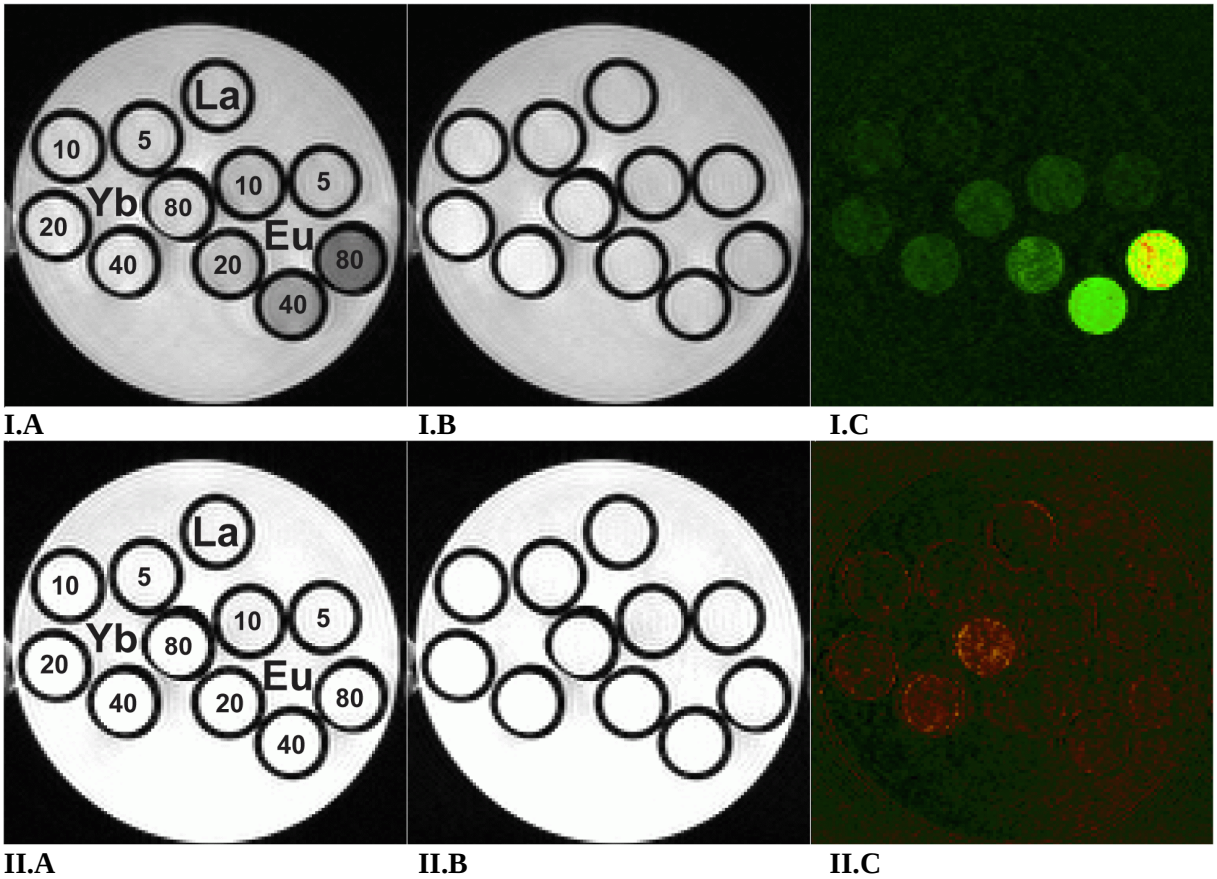

Fig. S14 MRI-CEST images of phantom consisting of one vial containing 80 mM aq. solution of [La(H_2O)(**L**^{1})] as a standard and five vials containing aqueous solution of [Eu(H_2O)(**L**^{1})] and [Yb(**L**^{1})] with different concentrations; pH = 7.4; concentrations (mM) are given as labels in figures **A**. Experimental conditions: RARE pulse sequence, B_0 = 4.7 T, B_1 = 20 μT, T = 293 K, satdly = 2 s, TR = 5 s, TE = 8.9 ms, scan time = 2 min. **I.A**: T_1-weighted image, satfrq = 34 ppm from the bulk water signal. **I.B**: T_1-weighted image, satfrq = –34 ppm from the bulk water signal. **I.C**: The difference between images **I.A** and **I.B** in false colours. **II.A**: T_1-weighted image, satfrq = 89 ppm from the bulk water signal. **II.B**: T_1-weighted image, satfrq = –89 ppm from the bulk water signal. **II.C**: The difference between images **II.A** and **II.B** in false colours.

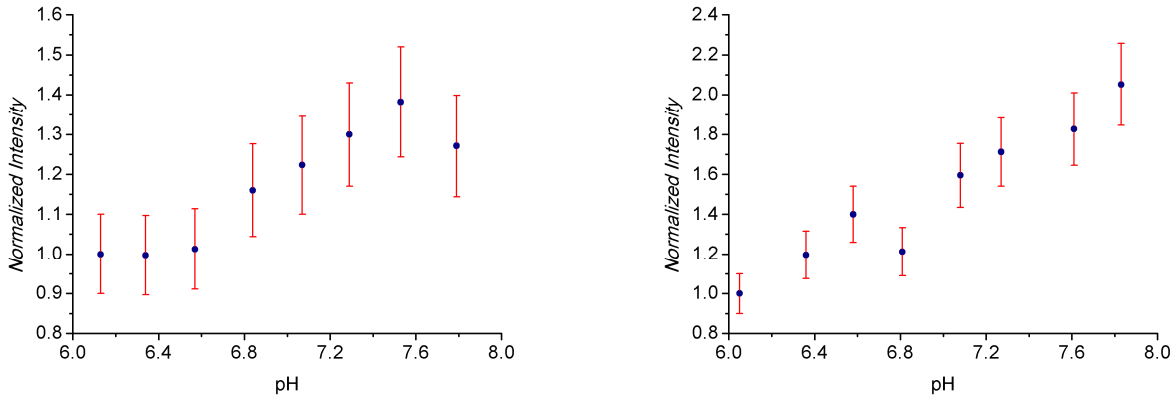

A **B**

Fig. S15 pH dependence of normalized intensity of the CEST effect (20 μT, MRI 4.7 T). **A**: [Eu(H_2O)(**L^1**)], data from Fig. 5-I.C. **B**: [Yb(**L^1**)], data from Fig. 5-II.C.

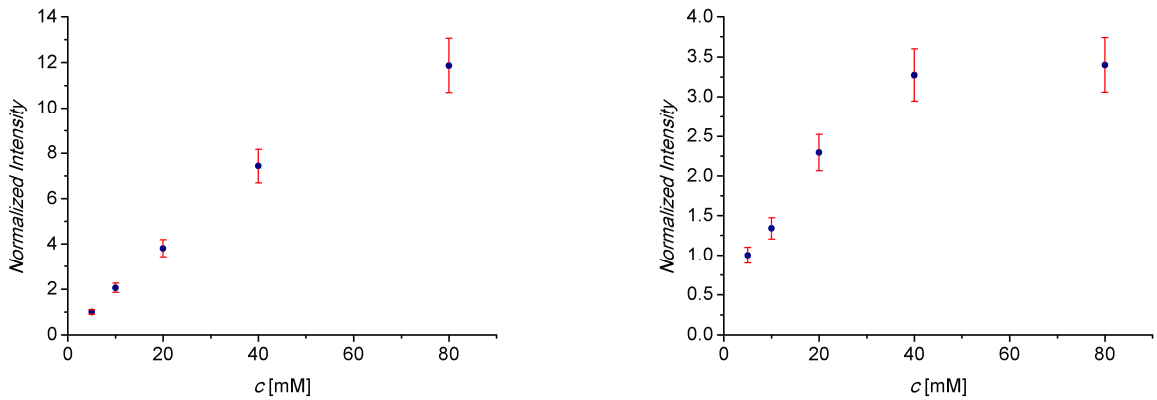

A **B**

Fig. S16 Concentration dependence of normalized intensity of the CEST effect (20 μT, MRI 4.7 T). **A**: [Eu(H_2O)(**L^1**)], data from Fig S14-I.C. **B**: [Yb(**L^1**)], data from Fig. S14-II.C.

Characterization ^{1}H and ^{13}C{^{1}H} NMR spectra of the ligands

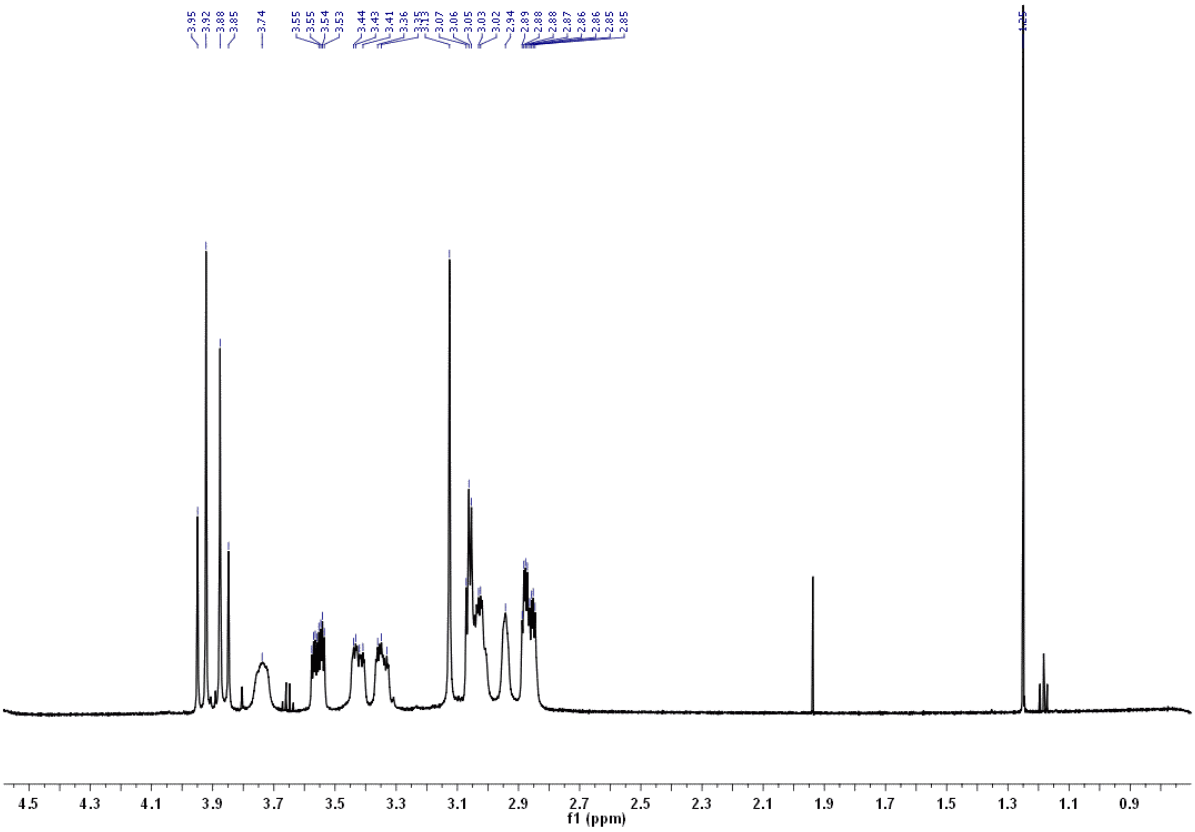

Fig. S17 ^{1}H NMR spectrum of H_3**L^{1}** in D_2O, pD = 5.4.

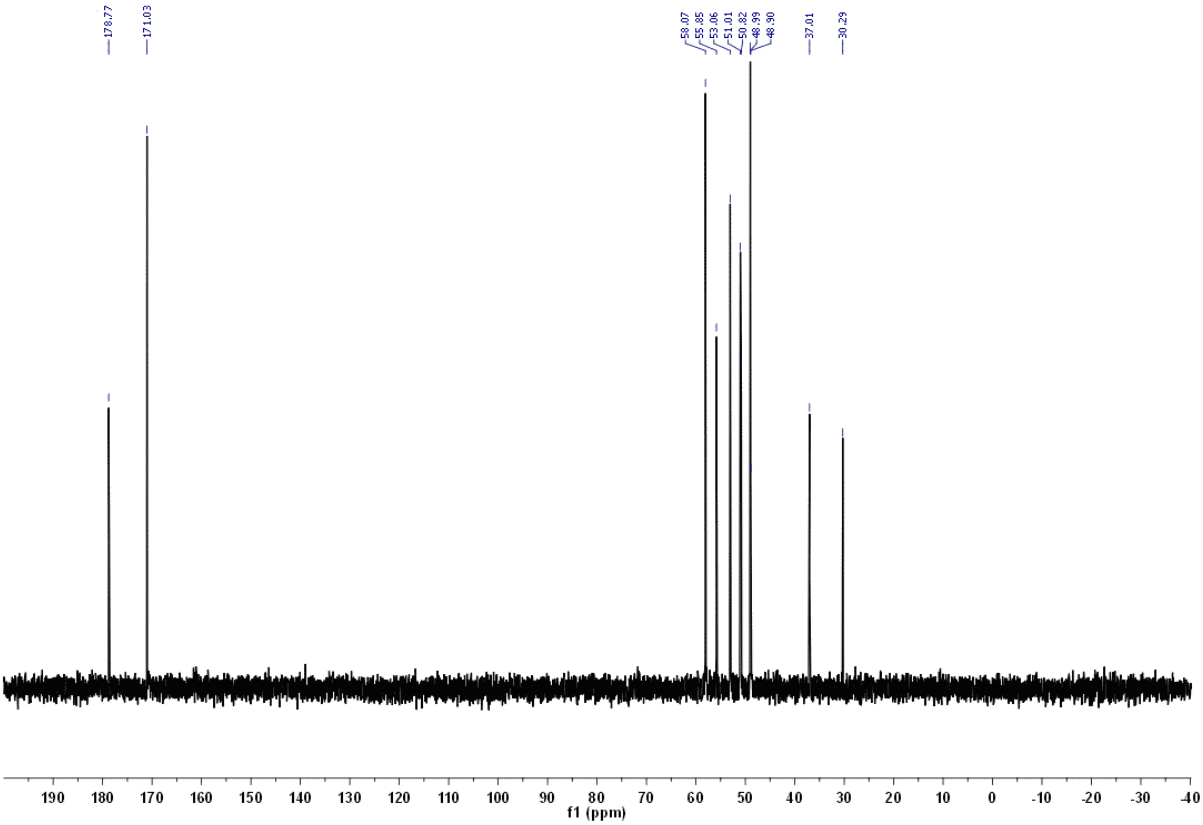

Fig. S18 ^{13}C{^{1}H} NMR spectrum of H_3**L^{1}** in D_2O, pD = 5.4.

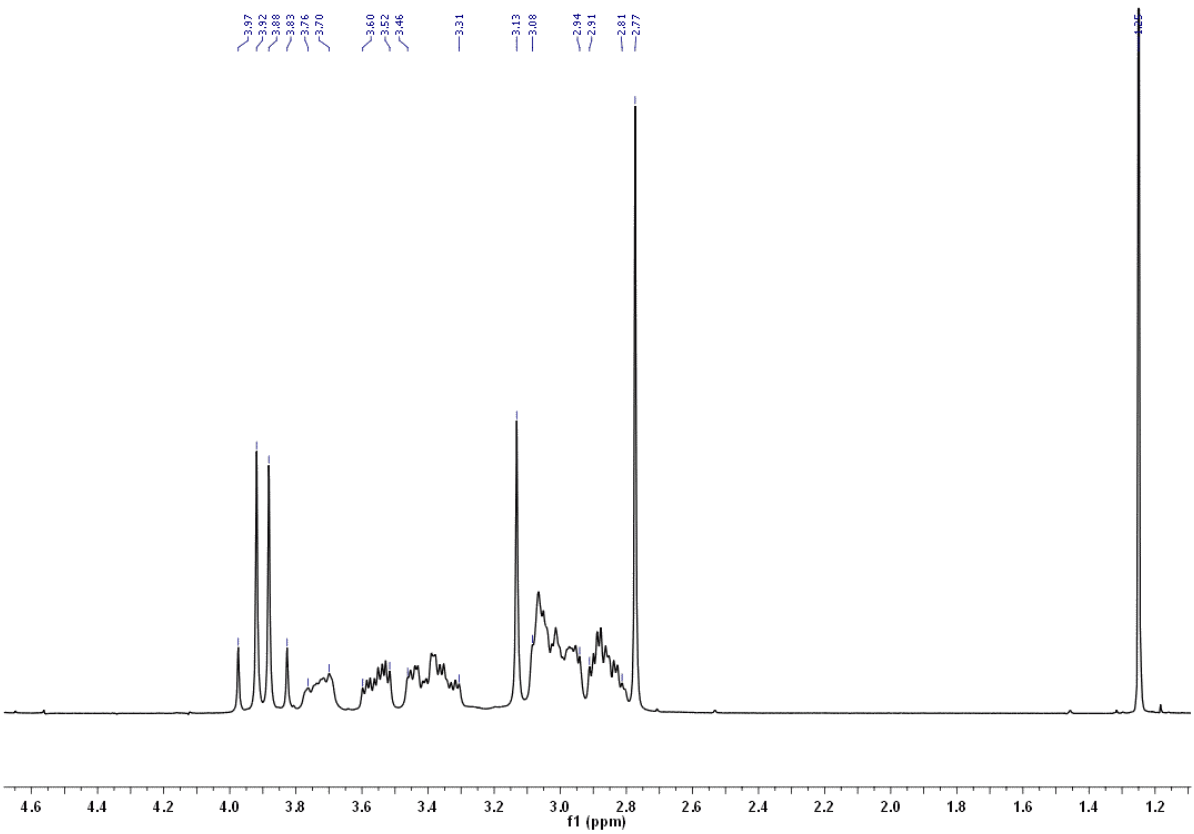

Fig. S19 ^{1}H NMR spectrum of $H_3\mathbf{L}^2$ in D_2O, pD = 5.3.

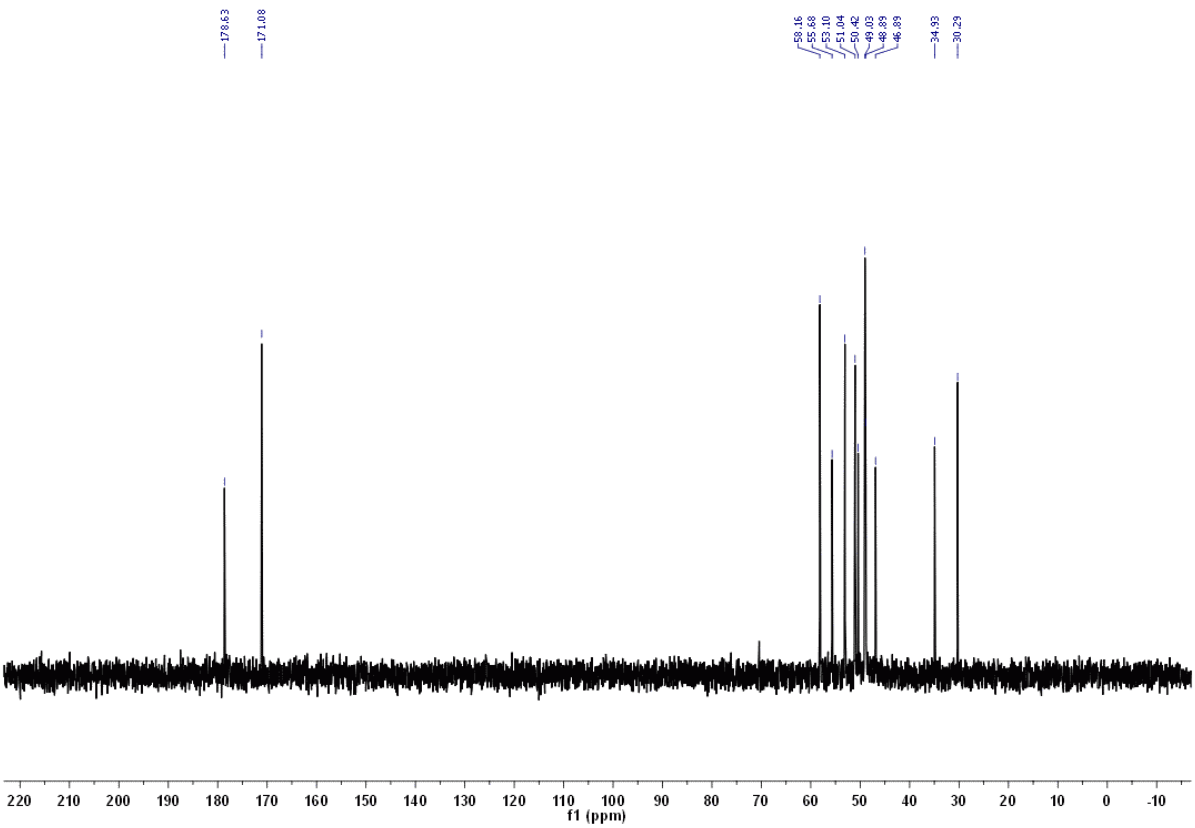

Fig. S20 ^{13}C NMR spectrum of $H_3\mathbf{L}^2$ in D_2O, pD = 5.6.

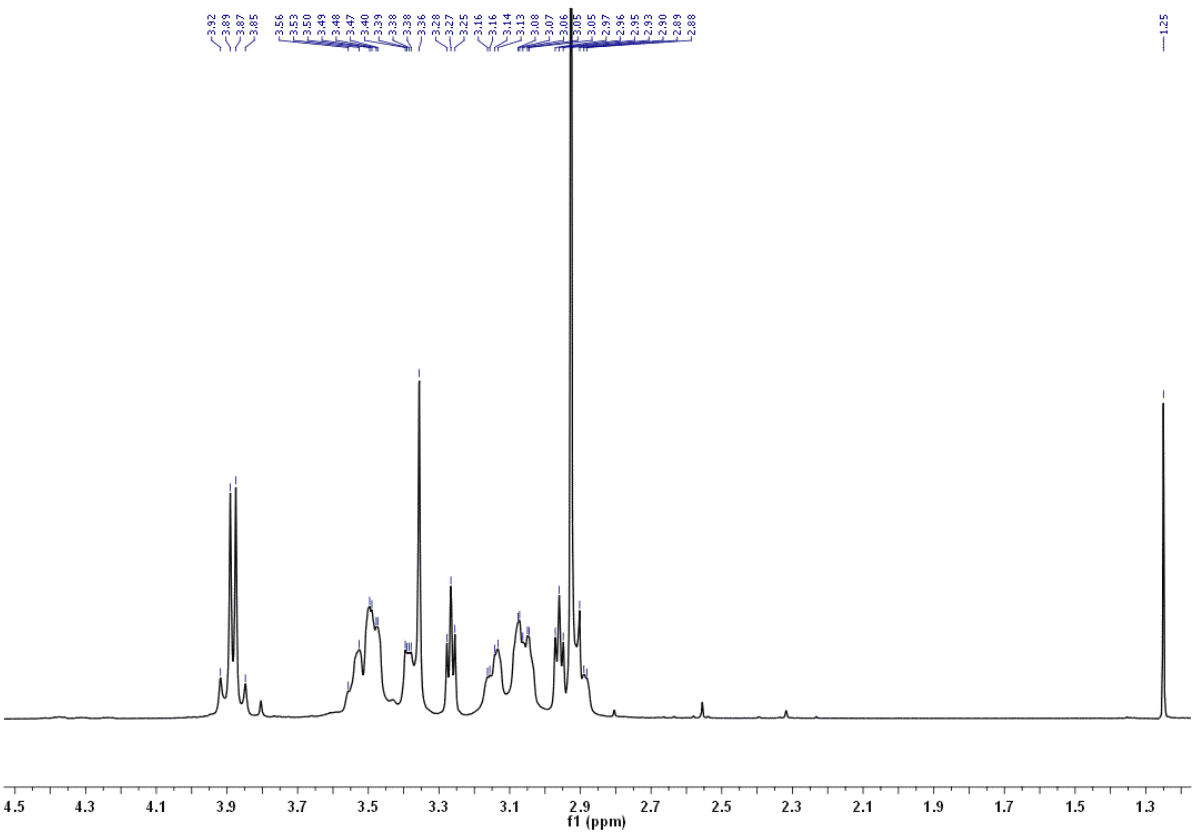

Fig. S21 ^{1}H NMR spectrum of H_3**L**^{3} in D_2O, pD = 4.8.

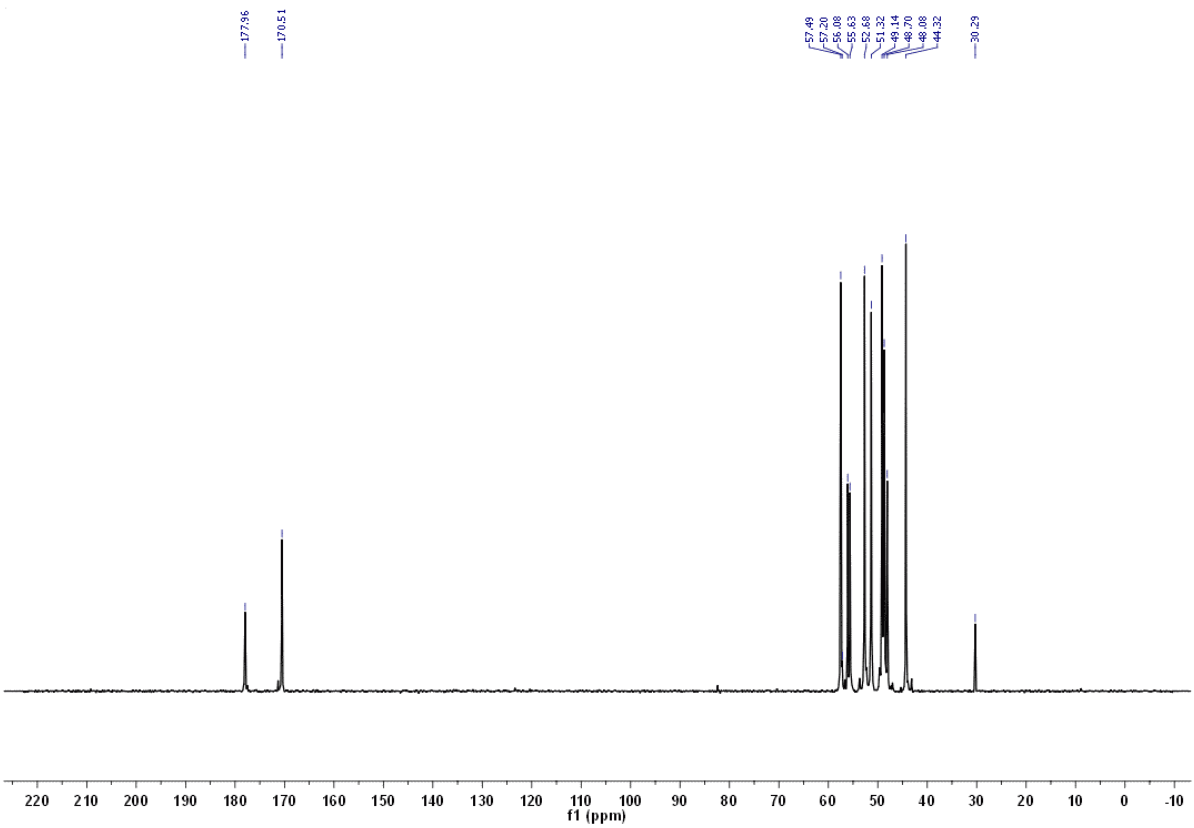

Fig. S22 ^{13}C{^{1}H} NMR spectrum of H_3**L**^{3} in D_2O, pD = 4.8.